Full Paper

Propellants, Explosives, Pyrotechnics

DOI: 10.1002/prep.201300074

Theoretical Prediction of Pressure and Temperature of an Aluminized High Explosive in Underwater Explosion

Vedula Dharma Rao,[a] Adapaka Srinivas Kumar,*[b] Kadiyam Venkateswara Rao,[b] Veerapaneni S. R. Krishna Prasad,[c] and Vepakomma Bhujanga Rao[d]

Abstract: The blast wave propagation in underwater explosion was studied. The shock propagation in water medium was different from that in air. The blast effect in water lasted longer and offered resistance to the expansion of hot gases and release of energy. A theoretical analysis of the expansion of blast wave in water was carried out and numerical results for pressures and temperatures were obtained as functions of distance and time by analytically solving the governing equations. The initial peak pressures of blast waves, which were required for theoretical analysis were calculated using the blast wave theory. Underwater blasts with different weights (0.045, 0.5, and 1.0 kg) of the aluminized high explosive HBX-3 were conducted to record pressure as a function of distance and time from the blast point. Theoretical results were compared with experimental data and empirical data for HBX-3 from literature. Since the measurement of pressure and temperature at close proximity of point of detonation is difficult, theoretical modeling of underwater blast is of significant importance.

Keywords: Aluminized high explosive · Blast underwater · Shock wave theory · Blast pressure · Temperature

1 Introduction

The detonation of high explosives is independent of the medium i.e., in air or in water. However, the expansion of blast wave differs depending on the medium into which the hot explosion gases expand. The properties of the medium such as density, surface tension, and viscosity influence the behavior of the blast wave. Unlike explosion in air, the energy released in underwater explosion is more or less equally distributed between the primary shock and the expanding gas bubble [1] called "Bubble Energy". In general aluminized high explosives such as HBX-3 or HBX-1 are filled in warheads and shells in military applications to inflict severe damage to the underwater targets. Aluminization of high explosives has been shown to enhance the underwater blast effect [2]. The peak pressure and temperature produced in the underwater blast can be estimated by calculating the stagnation pressure and temperature ahead of the shock wave [3,4]. The pressure behind the blast wave depends on the heat of detonation of the explosive [4,5].

2 Theoretical Analysis

In an explosion, the gas released by the blast uniformly expands in all directions. Hence the blast gas zone is assumed to be spherical in shape, filled with gas [6]. The shape of the blast wave also depends on the shape and weight of the explosive charge, the mode of initiation, and the properties of the ambient medium, among others [7]. Hence, a plane wave front is also considered to represent a limiting case of the analysis. The physical model showing the spherical and plane wave fronts is presented in Figure 1.

The task is formulated as follows: A spherical blast zone with an initial radius of R_0 is formed due to the explosion. The initial pressure and temperature of the gas in the blast zone are $p_{g,0}$ and $T_{g,0}$, respectively. Water is at a constant pressure equal to p_f and, if treated as an infinite heat sink, its temperature and density remain constant at T_f and ρ_f, respectively. Heat is dissipated from the blast zone by convection and radiation to the surrounding fluid. The pressure and temperature of the gas in the blast zone decrease as the wave front moves forward. The variables, which change

[a] *V. D. Rao*
Department of Mechanical Engineering
GVP College of Engineering
Visakhapatnam-530048, India

[b] *A. S. Kumar, K. V. Rao*
Naval Science and Technological Laboratory
Vigyan Nagar
Visakhapatnam-530027, India
**e-mail: adapakaeskay@yahoo.com*

[c] *V. S. R. K. Prasad*
Anil Neerukonda Institute of Technology and Science
Visakhapatnam-530054, India

[d] *V. B. Rao*
Defence Research and Development Organisation
DRDO Bhavan
New Delhi-110011, India

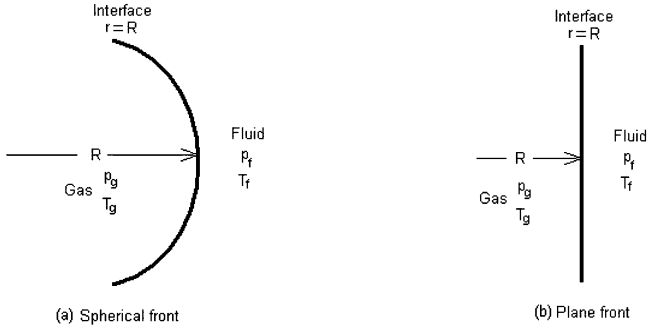

Figure 1. Physical model for movement of blast wave.

with time, are the radius of the blast gas sphere (R), pressure (p_g), temperature (T_g) and density (ρ_g) of the gas in the blast zone.

It is assumed that the gas in the blast zone behaves like a perfect gas and obeys the ideal gas law.

2.1 Motion of Water Adjacent to the Detonation Wave Front

The ambient liquid, i.e., water, which is adjacent to the blast wave front (at $r = R$) moves with the same velocity as the wave front moves. Thus, the velocity of the ambient liquid at $r = R$ is equal to u_i, where. $u_i = dR/dt$. However, the bulk liquid, which is away from the gas is at rest. Considering only radial displacements, the motion of the water is governed by (i) continuity and (ii) momentum balance equations in spherical coordinates as shown below.

$$\partial/\partial r\ (r^2 u) = 0 \tag{1}$$

$$\rho_f\left(\frac{\partial u}{\partial t} + u\frac{\partial u}{\partial r}\right) = -\frac{\partial p_f}{\partial r} + \mu_f \frac{1}{r^2}\frac{\partial}{\partial r}\left(r^2 \frac{\partial u}{\partial r}\right) - 2\mu_f \frac{u}{r^2} \tag{2}$$

On the right hand side of Equation (2), the terms containing coefficient μ_f are neglected, since the viscous force is by far low compared to inertial (LHS of Equation (2)) and pressure force (first term on RHS of Equation (2) under blast conditions). Thus, neglecting the viscous force terms and rearranging, Equation (2) becomes

$$\left(\frac{\partial u}{\partial t} + u\frac{\partial u}{\partial r}\right) = -\frac{1}{\rho_f}\frac{\partial p_f}{\partial r} \tag{3}$$

The boundary conditions (for $t > 0$) are listed as follows.

$$u = u_i \text{ at } r = R, \text{ and } u \to 0 \text{ as } r \to \infty \tag{4}$$

ρ_f and μ_f are the density and viscosity of the liquid, i.e., water respectively. The continuity equation Equation (1 is integrated using the boundary conditions, i.e., Equation (4) to yield the velocity profile in the liquid medium as given below.

$$u/u_i = (R/r)^2 \tag{5}$$

It can be observed that the velocity u is a function of both r and t. The terms in Equation (2) are integrated partially with respect to r yielding the following Equation (6).

$$\int_R^\infty \frac{\partial u}{\partial t} dr + \int_R^\infty u\frac{\partial u}{\partial r} dr = \frac{p_{f,i} - p_f}{\rho_f} \tag{6}$$

In the first term of LHS, u is differentiated first with respect to t and integrated next with respect to r. The order is changed to first integration and next differentiation by change of order of integration rule in mathematics as:

$$\frac{d}{dt}\int_R^\infty u\, dr + u_i\frac{dR}{dt} + \left[\frac{u^2}{2}\right]_{r=R}^{r=\infty} = \frac{p_{f,i} - p_f}{\rho_f} \tag{7}$$

Substituting the integration limits in the third term on LHS of Equation (7 for u (at $r = \infty$, $u = 0$ and at $r = R$, $u = u_i$), the following equation is obtained:

$$\frac{d}{dt}\int_R^\infty u\, dr + u_i\frac{dR}{dt} - \frac{u_i^2}{2} = \frac{p_{f,i} - p_f}{\rho_f} - \nu_f \left.\frac{\partial u}{\partial r}\right|_{r=R} - 2\nu_f \frac{u_i}{R^2} - \nu_f \int_R^\infty \frac{u}{r^2} dr \tag{8}$$

$p_{f,i}$ is the pressure of the fluid at the gas-to-liquid interface. The viscous force terms can be ignored for the present case of expansion into an open bulk liquid. Thus, Equation (8) reduces to the form given below:

$$\frac{d}{dt}\int_R^\infty u\, dr + u_i\frac{dR}{dt} - \frac{u_i^2}{2} = \frac{p_{f,i} - p_f}{\rho_f} \tag{9}$$

However, introducing the effect of surface tension, the force balance at the gas-to-liquid interface is given by

$$p_g = p_{f,i} + 2\sigma_s/R \tag{10}$$

p_g is the gas pressure and $p_{f,i}$ is the liquid pressure at the gas-to-liquid interface. σ_s is the surface tension of gas-to-fluid. The second term on right side of Equation (10) represents the surface tension force at the interface. The term $p_{f,i}$ appearing in Equation (9) is replaced with p_g by using Equation (10) and the resulting equation is given below.

$$\frac{d}{dt}\int_R^\infty u\, dr + u_i\frac{dR}{dt} - \frac{u_i^2}{2} = \frac{p_g - p_f}{\rho_f} - \frac{2\sigma_s}{\rho_f R} \tag{11}$$

The integral appearing in Equation (11) is evaluated by using the velocity profile given in Equation (5) to give the following equation:

$$\frac{d}{dt}(u_i R) + u_i\frac{dR}{dt} - \frac{u_i^2}{2} = \frac{p_g - p_f}{\rho_f} - \frac{2\sigma_s}{\rho_f R} \tag{12}$$

Considering the fact that $u_i = (dR/dt)$, Equation (12) can be written as follows:

$$R\frac{d}{dt}\left(\frac{dR}{dt}\right)+\left[\frac{dR}{dt}\right]^2+\frac{dR}{dt}\cdot\frac{dR}{dt}-\frac{1}{2}\left[\frac{dR}{dt}\right]^2=\frac{p_g-p_f}{\rho_f}-\frac{2\sigma_s}{\rho_f R} \quad (13)$$

After differentiation and simplification of Equation (13), the following equation is obtained.

$$\frac{d^2R}{dt^2}+\frac{3}{2R}\left(\frac{dR}{dt}\right)^2=\frac{p_g-p_f}{\rho_f R}-\frac{2\sigma_s}{\rho_f R^2} \quad (14)$$

The second term appearing on the right hand side of Equation (14) represents the surface tension force.

2.2 Heat Balance at the Gas-to-Fluid Interface ($r = R$)

Heat is transferred from the gas to the liquid by convection and radiation during the expansion of gas. A lumped heat capacity model is used for the blast zone. The equation of heat balance at the gas-to-water interface, i.e., at $r = R$, is as follows:

$$-c_{pg}\frac{d}{dt}\left[\rho_g\left(\frac{4}{3}\pi R^3\right)T_g\right]=\left(4\pi R^2\right)\left[h\left(T_g-T_f\right)+\varepsilon\sigma_r\left(T_g^4-T_f^4\right)\right] \quad (15)$$

As defined earlier, R is the distance of the gas-to-water interface measured from the blast point. The gases heat capacity is shown as c_{pg} and the convection heat transfer coefficient as h. The equation of heat balance can also be written as shown below considering plane front in the case of strong detonation wave.

$$-c_{pg}\frac{d}{dt}\left[\rho_g R_g T_g\right]=h\left(T_g-T_f\right)+\varepsilon\sigma_r\left(T_g^4-T_f^4\right) \quad (16)$$

Equation (15) and Equation (16) can both be represented by the unique equation given below:

$$\rho_g T_g\frac{dR}{dt}+\frac{R}{C}\frac{d}{dt}\left(\rho_g T_g\right)=-\frac{1}{c_{pg}}\left[h\left(T_g-T_f\right)+\varepsilon\sigma_r\left(T_g^4-T_f^4\right)\right] \quad (17)$$

where the curvature $C = 3$ for a spherical wave front and $C = 1$ for a plane wave front. A value between 1 and 3 represents a curved front.

Since the gas is assumed to obey ideal gas law, the following relation can be obtained between the gas density ρ_g and temperature T_g.

$$\frac{\rho_g}{\rho_f}=\frac{p_g}{p_f}\frac{T_f}{T_g} \quad (18)$$

ρ_f and p_f are the density and pressure of a reference gas, i.e., air at temperature T_f.

As the gas expands the pressure decreases and finally becomes equal to the pressure of the ambient air. The pressure and density of the ambient air are p_f and ρ_f, respectively. Polytropic expansion of gas is assumed in the blast zone. p_g, the gas pressure and ρ_g, the gas density are related as given by the following equation.

$$p_g/p_f=(\rho_g/\rho_f)^n \quad (19)$$

Initially, the gas pressure and density are p_{g0} and ρ_{g0}, respectively. The exponent of polytropic expansion, n can be obtained as follows.

$$n=\frac{\log\left(p_{g0}/p_f\right)}{\log\left(\rho_{g0}/\rho_f\right)}$$

Using Equation (18) and Equation (19), the gas pressure p_g and density ρ_g can be expressed as functions of the gas temperature T_g.

$$\frac{p_g}{p_f}=\left(\frac{T_g}{T_f}\right)^{n/(n-1)} \quad (20)$$

$$\frac{\rho_g}{\rho_f}=\left(\frac{T_g}{T_f}\right)^{1/(n-1)} \quad (21)$$

When Equation (20) and Equation (21) are considered to substitute for p_g and ρ_g in Equation (14) and Equation (17) respectively, the following differential equations are obtained:

$$\frac{d^2R}{dt^2}=\frac{p_f}{\rho_f R}\left[\left(\frac{T_g}{T_f}\right)^{\frac{n}{n-1}}-1\right]-\frac{2\sigma_s}{\rho_f R^2}-\frac{3}{2R}\left(\frac{dR}{dt}\right)^2 \quad (22)$$

$$\frac{dT_g}{dt}=-\frac{(n-1)}{n}\frac{C}{R}\left[\frac{1}{\rho_f C_{pg}}\left(\frac{T_f}{T_g}\right)^{\frac{1}{n-1}}\left\{h\left(T_g-T_f\right)+\varepsilon\sigma_r\left(T_g^4-T_f^4\right)\right\}+T_g\frac{dR}{dt}\right] \quad (23)$$

The initial conditions at $t = 0$ are as follows.

$$R = R_0 \text{ and } T_g = T_{g0} \quad (24)$$

then, from Equation (14), and since at $t = 0$, $d^2R/dt^2 = 0$,

$$\frac{dR}{dt}=\sqrt{\frac{2}{3\rho_f}\left(p_{g0}-p_f-\frac{2\sigma_s}{R_0}\right)} \quad (25)$$

p_{g0}, T_{g0} and R_0 in Equation (24) and Equation (25) are the peak over pressure, temperature, and radius of the gas sphere initially, i.e., at time zero. The values of all these

three parameters must be given, as they together form the initial conditions to solve the differential Equations (22) and (23).

Equation (22) and Equation (23) are solved numerically to obtain the radial distance R and gas temperature T_g as functions of time t making use of the initial condition given by Equation (24) and Equation (25). The gas pressure p_g and density ρ_g in the blast zone change during the expansion of the blast wave. Hence p_g and ρ_g at each time step are computed from Equation (20) and Equation (21) respectively. Thus, numerical results are obtained for pressure and temperature as functions of time and distance for different weights of explosives.

2.3 Evaluation of Initial Conditions

The values of p_{g0}, T_{g0} and R_0 are computed as follows.

The initial peak pressure p_{g0} and temperature T_{g0} are assumed to be equal to the stagnation pressure and temperature ahead of the blast wave. The stagnation pressure and temperature are independent of the fluid medium, in which detonation takes place. Hence, they are calculated from the principles of blast wave theory.

Since, it is considered that the initial peak pressure and temperature are equal to the stagnation pressure and temperature ahead of the wave respectively, $p_{g0} = p_{01}$ and $T_{g0} = T_{01}$. R_0 is the initial radius of the blast gas sphere and p_{g0} is the peak over pressure developed in it. The radius R_0 corresponding to the pressure p_{g0} is obtained from the experimental data for pressure versus distance for the blast of 1 kg explosive. The initial radii of the blast zone for different weights of the same explosive are calculated making use of scaling law [8].

3 Experimental Studies

Experiments were conducted to measure the blast pressures underwater with cylindrical HBX-3 (an aluminized high explosive) charges of diameter 30×30 mm, adjusting the weight to 0.045 kg. Firings were conducted with 0.045 kg HBX-3 charges at Naval Science and Technological Laboratory in a tank of dimensions 15×12×10 m depth [9]. Five firings were conducted to acquire consistent pressure data. A sensor with a measuring range of up to 70 MPa, (PCB 138A10) was placed at 0.5 m distance from the point of explosion and sensor with minimum range of 7 MPa, (PCB 138A01) was placed at 2.5 m. Sensors of 35 MPa, (PCB 138A05) range were placed at intermediate distances.

Firings were conducted at sea for higher weights i.e., 0.5 kg (diameter = 75×65 mm) and 1.0 kg (diameter = 90×90 mm) HBX-3 charges. Pressures were measured at 1.0, 2.0, 3.0, 4.0, and 5.0 m distances from the point of detonation at a depth of 5 m. Exhaustive arrangements were made to anchor a floating platform of 10×15 m width, to which the explosive charge and the blast sensors were fixed rigidly.

4 Results and Discussion

The experimental data and numerical results for pressures with distance obtained for different weights of HBX-3 were compared. In addition, temperatures were obtained from the theoretical equations. These results are presented as follows.

The numerical results obtained by solving Equation (22) and (23) for blast pressure of HBX-3 charges of 0.045, 0.5, and 1 kg are shown plotted against distance in Figure 2 using continuous line. The pressures measured at various distances from the blast point in underwater blasts of 0.045, 0.5, and 1 kg of cylindrical cast HBX-3 charges are also shown in Figure 2. The experimental pressures were measured up to 2.5 m in the case of 0.045 kg charge and up to a distance of 5 m in the case of 0.5 and 1 kg of HBX-3. Here, it is observed that the experimental pressure values and the pressure values obtained from empirical equations agree well with the theoretical values for shape factor value C = 1.2. Figure 2 also shows the blast pressures calculated from the following empirical equation (shown as circles) for HBX-3 [10].

$$P = 50.3\ (1/Z)^{1.13} \text{ for } 3.4 \leq P_{max} \leq 60 \qquad (26)$$

where P is the maximum pressure in MPa and Z is the scaled distance ($R/W^{1/3}$) in m $kg^{-1/3}$.

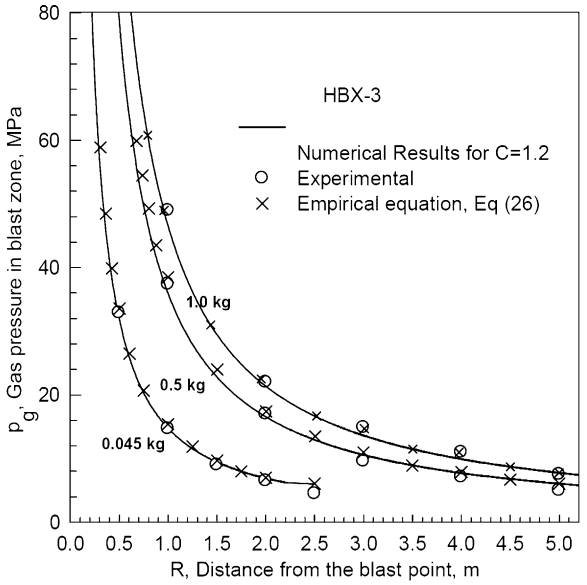

Figure 2. Comparison of theoretical results of gas pressure in blast zone for C = 1.2 with experimental data and empirical equation, Equation (26) for 0.045, 0.5, and 1.0 kg HBX-3.

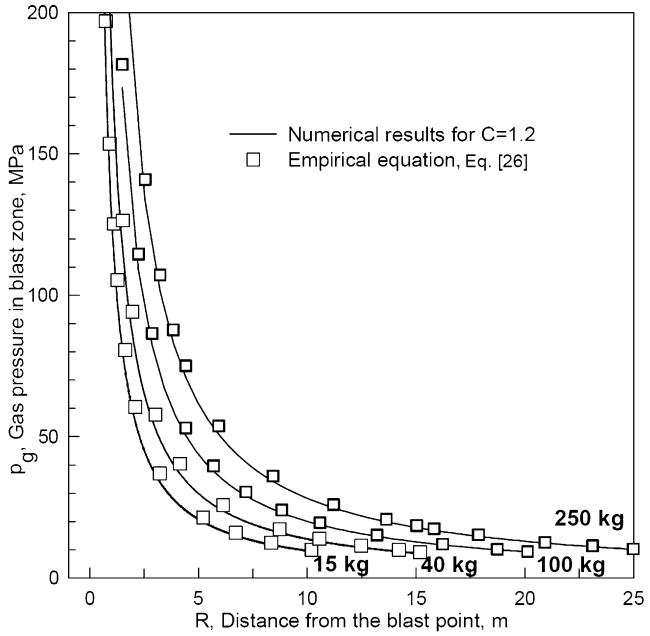

Figure 3. Comparison of theoretical results of gas pressure in blast zone for C = 1.2 with empirical equation, Equation (26) for 15, 40, 100, and 250 kg HBX-3.

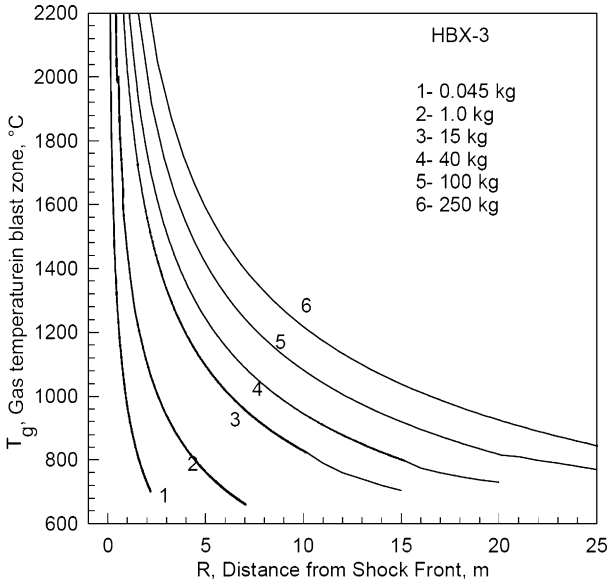

Figure 4. Variation of blast gas temperature with distance during expansion of blast wave for 0.045, 1, 15, 40, 100, and 250 kg HBX-3.

It can be observed from Figure 2 that the experimental data and numerical results of the present theoretical analysis agree well over the entire range of distance. The results computed from the empirical equations from literature also agree well with the experimental data and numerical results, thus confirming the validity of the experimental and the theoretical studies carried out presently.

Pressures are also obtained from the theoretical analysis for higher weights viz., 15, 40, 100, and 250 kg HBX-3 and the same are shown in Figure 3 along with a comparison with the pressures calculated from empirical equation, Equation (26). The theoretically computed pressures are shown in Figure 3 for 15 kg and 40 kg HBX-3 charges up to 10 m and 15 m distance respectively, from the point of detonation. This figure shows the pressure values for 100 and 250 kg HBX-3 up to distances of 20 m and 25 m, respectively. The empirical equation, which is useful by virtue of its simplicity, continues to give points in close agreement with the above analytical theory (where C = 1.2) as can be observed from the plot. An important outcome of the present theoretical analysis is that it is able to predict pressures over a very large range of weights of HBX-3, viz., from 0.045 to 250 kg as can be evinced from Figure 2 and Figure 3.

It is usually difficult to measure temperatures in experiments conducted for the underwater blast of explosives. Under these circumstances the present theoretical study assumes immense importance, since the temperature as a function of distance (and time) is obtained in the theoretical results as a natural consequence. When an explosion takes place underwater, the gaseous combustion products at high temperature and pressure are captured in the form of a gas bubble in the infinite water medium. Lethality of a weapon depends on pressure and energy contained in the bubble. Since pressure and temperature complement each other mutually, higher the pressure or temperature higher will be the lethality. Thus, lethal range of the weapon enhances. The present study can help in estimation of lethality more accurately. Variation of gas temperature with distance for 0.045, 1.0, 15, 40, 100, and 250 kg HBX-3 is shown in Figure 4. The temperature falls from 2200 °C to about 700 °C within a distance of 2 m from the point of explosion for 0.045 kg HBX-3 underwater. Similar trends are observed with higher weights of explosive also viz., 1.0, 15, 40, 100, and 250 kg of HBX-3. Data are plotted for different distances increasing from 2 to 25 m distances depending on the weight of explosive varying from 0.045 kg to 250 kg of HBX-3. As can be seen from the plot, the temperature falls from 2200 °C (at 1 m) to less than 770 °C with in a distance of 12 m for 15 kg HBX-3, while for 40 kg, it falls to about 875 °C at the same distance. Decay of temperatures with distance for 100 kg and 250 kg HBX-3 also follow similar trend. However, the distance at which the temperature reaches to 800 °C is accordingly higher for 100 kg and 250 kg explosive as compared to 15 kg and 40 kg explosive.

5 Conclusions

Theoretical results of pressures obtained for seven different weights (0.045, 0.5, 1.0, 15, 40, 100, and 250 kg) of HBX-3 are in well agreement with the results of empirical data.

Theory also agrees well with the experimental values of pressures for 0.045, 0.5, and 1.0 kg of HBX-3. The analytical theory can be used to predict pressures at very close distances from point of detonation for a wide range and various weights of explosives. The authors verified the validity of the theory for weights ranging from 0.045 kg to 250 kg. Variation of pressure with time can also be predicted using this model. In addition, as a natural consequence, the present analytical theory also predicts temperature in the blast zone varying with distances. Thus, the model can also compliment prediction of lethality of an underwater weapon, deployed against static and dynamic underwater targets.

Symbols and Nomenclature

HBX-3	RDX/Al/TNT/WAX/$CaCl_2$: 31/35/29/5/0.5
HBX-1	RDX/Al/TNT/WAX/$CaCl_2$: 40/17/38/5/0.5
RDX	Cyclo trimethylene trinitroamine
TNT	Trinitrotoluene
Al	Aluminum
Q	Heat of detonation [kJ kg^{-1}]
C	Curvature factor defined in Equation (11), C = 3 (spherical front), C = 1 (plane front)
g	Gravitational constant [m s^{-1}]
h	Convection heat transfer coefficient [W m^{-2} K^{-1}]
k	Thermal conductivity [W m^{-1} K^{-1}]
n	Exponent of polytropic process as defined in Equation (19)
p	Pressure [N m^{-2}]
r	Position coordinate [m]
R	Distance from blast point to gas-to-fluid interface [m]
Z	Scaled distance [$R/W^{1/3}$]
t	Time [s]
T	Temperature [K]
u	Velocity of fluid [m s^{-1}]

Greek Symbols

ε	Emissivity
ρ	Density [kg m^{-3}]
ρ_g	Density of gas at temperature T_f [kg m^{-3}]
σ_s	Surface tension [N m^{-1}]
σ_r	Stefan-Boltzmann constant, 5.67×10^{-8} W m^{-2} K^4
μ_f	Viscosity [kg s^{-1} m^{-1}]
c_{pg}	Heat capacity [J K^{-1}]
υ	Kinematic viscosity [m^2 s^{-1}]

Subscripts

0	Inlet
f	Fluid
g	Gas
i	Gas-to-fluid interface

Acknowledgments

The authors thank Prof. P. K. Sarma for his help in theoretical analysis. The authors thank Dr. A. Subhananda Rao, Director, High Energy Materials Research Laboratory, Pune for providing explosives. The Scientists/Officers of NSTL, Visakhapatnam and HEMRL, Pune who helped in conduct of the experiments are gratefully acknowledged. The authors also thank Mr. A. Jagannadham, NSTL, Visakhapatnam who helped with the preparation of this paper.

References

[1] M. Held, The Physical Phenomena of Underwater Detonation, *J. Explos. Propellants* **1997**, *13*, 1–12.
[2] E. Stromsoe, S. W. Eriksen, Performance of High Explosives in Underwater Applications. Part 2: Aluminized Explosives, *Propellants Explos. Pyrotech.* **1990**, *15*, 52–53.
[3] A. H. Shapiro, *Compressible Fluid Flow*, John Wiley & Sons, Hoboken, NJ, Vol. 1, **1953**.
[4] P. H. Oosthuzen, E. C. William, *Compressible Fluid Flow*, McGraw-Hill Publication, **1997**.
[5] V. Krishna Mohan, B. Tang Tong, Explosive Performance Potential – A New Definition, *Propellants Explos. Pyrotech.* **1984**, *9*, 30–36.
[6] B. D. Khristoforov, Effect of Properties of Source on the Action of Explosions in Air and Water, *Combust. Explos. Shock Waves (Engl. Transl.)* **2004**, *40*, 714–719.
[7] Robert, H. Cole, *Underwater Explosions*, Dover Publications, New York, NY, **1965**, 122.
[8] W. E. Baker, *Explosions in Air*, University of Texas Press, Austin, TX, **1973**.
[9] A. S. Kumar, V. B. Rao, R. K. Sinha, A.S Rao, Evaluation of Plastic Bonded Explosive (PBX) Formulation Based on RDX, Aluminium and HTPB for Underwater Applications, *Propellants Explos. Pyrotech.* **2010**, *35*, 359–364.
[10] S. M. Kaye, H. L. Herman, *Encyclopedia of Explosives and Related Items*, PATR 2700, 10, Weapon System Laboratory, Dover, New Jersey, **1983,** U48.

Received: June 27, 2013
Revised: September 26, 2013
Published online: December 2, 2013

